

## Article

# Thermodynamic Modeling and Exergoenvironmental Analysis of a Methane Gas-Powered Combined Heat and Power System

Michael Adedeji<sup>1</sup>, Muhammad Abid<sup>2</sup>, Humphrey Adun<sup>1,\*</sup>, Ayomide Titus Ogungbemi<sup>1</sup>, David Alao<sup>1</sup> and Juliana Hj Zaini<sup>2</sup>

<sup>1</sup> Department of Energy Systems Engineering, Cyprus International University, Mersin 10, Nicosia 99258, Turkey

<sup>2</sup> Department of Energy Systems Engineering, Faculty of Integrated Technologies, Universiti Brunei Darussalam, Jalan Tungku Link BE, Bandar Seri Begawan 1410, Brunei

\* Correspondence: hadun@ciu.edu.tr; Tel.: +90-5488243140

**Abstract:** A combined heat and power (CHP) system powered by methane gas is modelled and analyzed in this study. The Thermolib MATLAB extension is used to model the system by graphically connecting the Thermolib standard components through fluid flows. An exergoenvironmental analysis is also performed using EES. The results show that, for an input thermal energy rate of 29.9 MW, the Brayton and Rankine cycles generated 9.8 MW and 7.5 MW of net power, respectively. The heat pump was also able to supply 1.4 MW as its output. The total energy efficiency of the cogeneration system was 62% with the Brayton cycle working at 33%, the Rankine cycle at 36%, and the ammonia heat pump at a coefficient of performance (COP) of 9.1. The system also achieved an overall exergy efficiency of 78%. Furthermore, the system was examined at different levels by varying input parameters such as the pressure ratio of both the Brayton cycle and the heat pump, the pressure of the steam in the Rankine cycle, and the inlet energy from the combustion chamber of the system. The exergoenvironmental modeling of the system showed that the exergy stability factor and exergetic sustainability index increased from 0.41 to 0.47 and from 0.6 to 0.64 with increasing inlet combustion energy; this can be seen as a good indicator of its stability and sustainability.



**Citation:** Adedeji, M.; Abid, M.; Adun, H.; Ogungbemi, A.T.; Alao, D.; Zaini, J.H. Thermodynamic Modeling and Exergoenvironmental Analysis of a Methane Gas-Powered Combined Heat and Power System. *Appl. Sci.* **2022**, *12*, 10188. <https://doi.org/10.3390/app121910188>

Academic Editors: Alexander Eremin and Xiaolin Wang

Received: 8 July 2022

Accepted: 7 October 2022

Published: 10 October 2022

**Publisher's Note:** MDPI stays neutral with regard to jurisdictional claims in published maps and institutional affiliations.



**Copyright:** © 2022 by the authors. Licensee MDPI, Basel, Switzerland. This article is an open access article distributed under the terms and conditions of the Creative Commons Attribution (CC BY) license (<https://creativecommons.org/licenses/by/4.0/>).

**Keywords:** cogeneration; thermal energy; exergoenvironmental analysis; simulation

## 1. Introduction

Energy is a crucial item in our daily life for almost everything, and its production, conversion, and uses closely affect the environment and sustainable development. Humanity has long depended on energy in the form of power and heat, among others, and has devised means of supplying these using power generating systems and heat producing systems which convert a primary energy source into these outputs. Cogeneration or combined heat and power (CHP) plants, which produce more than the output from a single energy source, provide an attractive approach due to their higher thermal efficiency than individual systems and lower environmental impact. This has enabled the widespread use of these systems all around the world.

Energy analysis, which is based on the first law of thermodynamics, provides a means to analyze the performance of thermal systems according to certain design parameters and operating conditions. However, it does not provide a clear picture of thermodynamic efficiency and losses. Exergy analysis overcomes these deficiencies and can help identify pathways to sustainable development [1]. Exergy is a useful tool for determining the location, type, and true magnitude of exergy losses, which appear in the form of either exergy destruction or waste exergy emission. Therefore, exergy can assist in developing strategies and guidelines for more effective use of energy resources and technologies [2]. Exergoenvironmental analysis likewise is an analysis method coupling the principles of

thermodynamics and environics to assess the environmental impacts of the system in the view of thermodynamics [3].

Numerous studies have utilized exergy and exergoenvironmental analysis to examine the inefficiencies and the impact of energy systems on the environment. Karklina et al. [4] performed an exergy analysis in a biomass combined heat and powerplant in Jelgava, finding about 64% of exergy destruction just in the steam generator, followed by the heat exchangers of the district heating system. Ahmadi et al. [5] performed an energy and exergoenvironmental analysis on a system designed to produce multiple outputs. The results showed that the system, compared to individual systems, exhibited higher exergy efficiencies and lower environmental impacts, suggesting that multigeneration can help mitigate greenhouse gas emissions. Eduardo et al. [6] also performed an exergy and exergoenvironmental analysis of a solar hybrid trigeneration system. Their results led to the conclusion that the solution pump and high-pressure generator are the highest sources of inefficiency in the system, and the exergoenvironmental performance of the system can be improved by enhancing the exergy efficiency of these components. Ratlamwala et al. [7] performed a comparative environmental compact assessment of two separate hydrogen and cooling cogeneration systems. Indices such as the environmental impact factor, environmental impact coefficient, environmental impact index, environmental impact improvement, exergetic stability factor, and exergetic sustainability factor were used in a bid to determine which system has a more favourable impact on the environment. The electrolyzer was found to score better than the steam methane reforming hydrogen production method.

Several models of powerplants with different energy sources, both conventional and renewable sources, have been designed and developed using software for powerplant simulation that can simulate the systems in both steady and dynamic states. Many researchers make use of commercial software such as Aspen Plus Dynamics, APROS (Advanced Process Simulation Software), ThermoSysPro (Modelica-based) library developed by EDF, SimECS developed by Delft University of Technology and used for dynamic simulation of energy conversion system [8], Dymola, and VMGSim.

Different models of powerplants and their components have been designed and simulated by researchers with their steady and transient performance observed and analyzed. Alobaid et al. [9] made use of APROS software in designing a simulation model of static and dynamic characteristics. The designed model is applied to the study of the start-up process in power plants. Starkloff et al. [10] developed a full-scale dynamic model of a large-scale coal-fired powerplant. It investigated operation flexibility by making use of APROS. A simulation model of the dynamic operation of a regenerative gas turbine was developed by [11], which analyzed the dynamic characteristics of a small engine with a static recuperator. Other researchers performed the numerical analysis of combined cycle powerplants and validated the models against measurements at different steady states [12,13].

Several other studies have been conducted on the dynamic modelling of powerplants. Maffezzoni [14] performed an analysis which identified those basic concepts that are usually accepted to form the primary state of the knowledge in powerplant modelling and simulation. Lu [15] explained the modelling techniques and carried out an analytical study on the fundamental steady state and dynamic models for powerplant components. In his study, a 677 MW coal and gas powerplant was modelled using dynamic characteristics with MATLAB and SIMULINK. Colonna and Putten [16] analyzed and validated SimECS, which is dynamic modelling software for energy systems. SimECS then underwent development at the Delft University of Technology and was continually utilized in the modelling of small steam cycle powerplants [17]. Due to the transient operation of dynamic models, it became important to utilize dynamic simulation tools for modelling such systems (powerplants). Celis et al. [18] carried out a dynamic model simulation study on a steam turbine for a full-scope powerplant simulator. Oko and Wang [19] also made use of Gproms in designing a dynamic model of a 500 MW coal-fired subcritical powerplant. A 5% correction error

was recorded in the model validation, in comparison with the actual plant measurement. Wang et al. [20] developed dynamic models of a 660 MW supercritical unit with the GSE software to obtain the energy consumption characteristics of power units during transient cycling processes. The study considered the heat storage, control systems unit, and energy utilization of the powerplant. The different outputs of the steady-state condition and at different cycling rates were measured and compared. The system showed an increment in the standard coal consumption rate (SCCR) by 3.57 g/kWh in the cycling rate as compared to the steady-state model. In their research, Powell and Edgar [21] developed a dynamic simulation of a thermal energy storage system incorporated into a parabolic trough concentrated solar power (CSP) system. The thermal storage system (TSS) utilized the two-tank direct method. Xu et al. [22] considered all the working parameters of TSS of a 1 MW solar tower powerplant by using modular modelling methods. Chen et al. [23] developed an integrated powerplant model. Steady-state data of a subcritical powerplant with reheat and regenerative cycle was used in validating the model designed. The nominal power and efficiency of the system were 605 MW and 38.3%, respectively. Liu et al. [24] worked on concentrated solar power plants by providing a comprehensive summary of both in operation and under construction.

There have been numerous studies in the literature on combined heat and power systems; however, this paper contributes to the literature by expanding on the effects of different variables such as the pressure ratio for improving the performance of these systems. The significance includes a better understanding of the practical implementation of multigeneration systems. Furthermore, trigeneration can be understood through exergoenvironmental analysis, although these analyses have not yet been published, particularly for systems based on organic Rankine cycles. The novelty of this study also stems from the utilization of the Thermolib software for the analysis, as few studies have utilized its robust computing capacity for such analyses. The present paper analyzes a combined heat and powerplant using the Thermolib extension library in MATLAB/Simulink. The behavior of the system analyzed consists of a Brayton cycle using methane gas as fuel, Rankine cycle, and ammonia heat pump, with the system performance and efficiency observed for varied component parameters. The effect of varying the pressure ratio of the Brayton cycle on the performance of the Brayton cycle, the combined gas and steam cycles, and the overall system is investigated. Similarly, the effect of varying the Rankine cycle turbine inlet pressure on the performance of the Rankine cycle and the overall system is investigated. The heat pump compressor pressure ratio is also varied to analyze its impact on the performance of the heat pump and the total system. The effect of varying the inlet energy from the combustion chamber of the Brayton cycle on the performance of each of the components is studied. Furthermore, its effect on the total system is analyzed. Lastly, an exergoenvironmental analysis is performed using the engineering equation solver (EES) to examine its environmental usefulness, appropriateness, and stability.

## 2. Materials and Methods

The system consists of a gas turbine (Brayton) cycle as the topping cycle, a steam turbine (Rankine) cycle next below it, and then an ammonia heat pump that can be used for space heating, as displayed in Figure 1. Air at ambient temperature and pressure (state 1) is fed into the compressor of the gas turbine cycle. The air at high pressure (state 2) is then transferred into the mixing chamber where it is mixed with the fuel (state 3) needed for the gas power plant. Methane gas ( $\text{CH}_4$ ) is used from the Thermolib setup block, and its data are loaded into the MATLAB workspace. In the presence of air and at constant pressure, the fuel is burnt in the combustion chamber. This gives rise to a high-temperature gas (state 4) which is transferred into the turbine. Inside the turbine, the high-temperature gas expands and produces power or electricity. The exhaust gas (state 5) which leaves the turbine possesses considerably high thermal energy, i.e., it leaves at a very high temperature (about 650 °C); therefore, it is used as the heat source for the steam cycle.

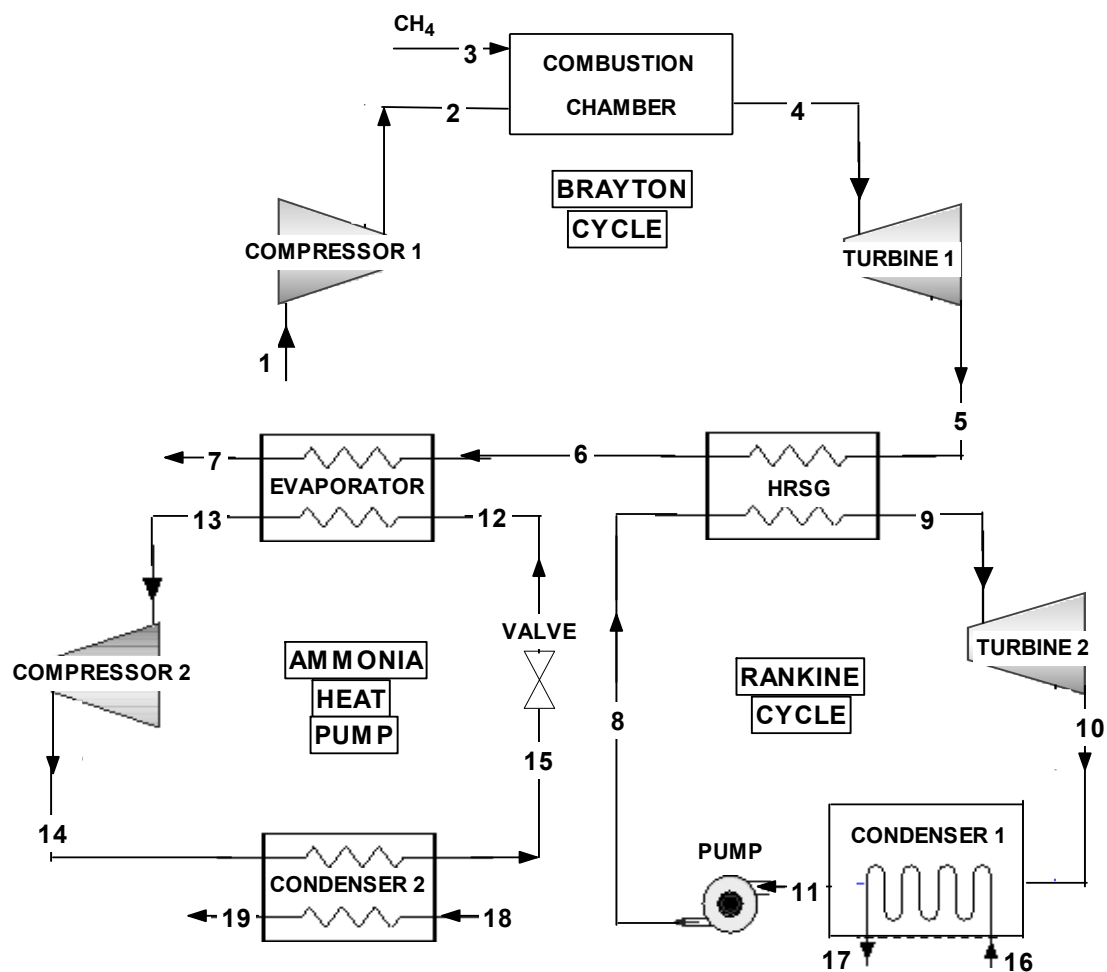


Figure 1. Model diagram of the multigenerational system.

The exhaust gas from the gas cycle is transferred into the steam cycle by entering the heat recovery steam generator (HRSG). The water from the steam cycle (state 8) which enters the HRSG comes out as steam with high pressure and temperature (state 9). This steam enters the steam turbine and expands, thereby generating additional electricity. The steam leaving the turbine after expansion (state 10) is then passed through a condenser where it is cooled down into a saturated liquid, using a stream of water/air (states 16 and 17). The saturated liquid (state 11) leaving the condenser is then pumped into the HRSG to recycle the process. The exhaust gas after leaving the heat recovery steam generator (state 6) still possesses enough energy which is fed into the ammonia heat pump. Here, the ammonia flowing into the evaporator (state 8) receives heat from the exhaust gas and leaves at a higher temperature (state 13). The ammonia is then compressed into the high-pressure level of the heat pump, thereby causing its temperature to be further increased. The hot fluid is then passed through the condenser where it exchanges heat with the process air at ambient temperature (state 18), which leaves it at a much higher temperature (state 19). The ammonia leaving the condenser (state 14) is then passed through an expansion valve to reduce its pressure (state 12) to that of the HRSG.

### 2.1. The Model and Components

The information regarding the components of the proposed system is presented in this section.

### 2.1.1. Methane Gas

The fossil fuel is combusted in the combustion chamber part of the gas cycle section of the system. This, therefore, entails the addition of heat through a chemical reaction. The combustion process of natural gas is less complex compared to that of coal and biomass. The model of the combustion chamber has the oxidizer inlet where the compressed wet air enters the chamber. It also has a fuel inlet where the natural gas used (methane) enters and the flue gas outlet.

The combustion chemical reaction in the combustion chamber assumes the following form:



In a real practical reactor or combustion chamber, other gaseous byproducts are given out such as nitrogen, as air contains other elements other than oxygen.

Equation (2) is an expression of the mass balance.

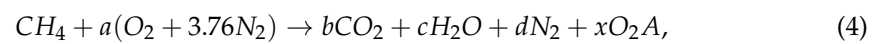
$$\dot{m}_{out,fg} = \dot{m}_{in,air} + \dot{m}_{in,fuel}. \quad (2)$$

Equation (3) is an expression of the energy balance.

$$\dot{m}_{out,fg}h_{out,fg} = \dot{m}_{in,air}h_{in,air} + \dot{m}_{in,fuel}LHV_{fuel}, \quad (3)$$

where the subscript *fg* refers to flue gas, and LHV represents the lower heating value of the fuel.

Upon ascertaining the fuel and mass flow rates entering the combustion chamber, the air-to-fuel ratio can be computed. According to [25], the reaction assumes the following form:



where the *x* term ensures the availability of excess oxygen in the exhaust gases released at the outlet of the combustion chamber.

### 2.1.2. Brayton Cycle

A compressor is a turbo machine. The compressor increases the pressure of the compressible fluids. The ratio of the outlet pressure to the inlet pressure is known as the compressor pressure ratio, which shows the increase in pressure in the system. The mass balance of the compressor is defined as

$$\dot{m}_{in} = \dot{m}_{out}. \quad (5)$$

The energy balance is given as

$$\dot{m}_{in}h_{in} = \dot{m}_{out}h_{out} + P. \quad (6)$$

In order to calculate the required performance,

$$P = \dot{m}C_p(T.)T_{ini}\eta_{comp}, \quad (7)$$

where  $C_p$  stands for the specific heat capacity of air and at the average temperature, and

$$T. = \frac{(T_{in} + T_{out})}{2}. \quad (8)$$

For isentropic efficiency of the compressor,

$$\eta_{isen,comp} = \frac{(h_{out,isen} - h_{in})}{(h_{out} - h_{in})}. \quad (9)$$

A combined cycle powerplant comprises the gas turbine as a section of the system. The enthalpy of the flue gas is transformed into mechanical energy by the gas turbine, which in turn drives the generator that produces the electrical energy. The other output of the gas turbine allows the waste heat from the turbine to pass out. This waste heat can be passed out to a heat recovery steam generator (HRSG) which is used to produce steam, as well as drive a steam turbine. Various fuels can be used to operate a gas turbine. These fuels include natural gas (which is used for the system in this paper), crude oil, and biogas. The fuel range of a gas turbine can be extended to include coal and also biomass by applying the integrated gasification combined cycle (IGCC) [26].

Considering that heavy-duty gas turbines have a much higher inlet temperature, in comparison with the steam turbine, they need cooling of their first row of blades. Due to this cooling, the mathematical model of the gas turbine is different from that of the steam turbine. Hence, the whole gas turbine has to be separated into different sections due to the presence of air cooling. The combustion gas mixes with the air cooling from a section, and this is computed in the mass balance equation of the turbine section. Founded on actual data, Wang and Leithner [27] proposed a formula for the calculation of the mass flow of the cooling air needed at nominal load:

$$\dot{m}_{cool} = \dot{m}_{air} \left( 3.1817 \cdot 10^{-4} T_{inl} - 0.2454 \right), \tag{10}$$

where  $\dot{m}_{air}$  is the total air mass flow rate, while  $T_{inl}$  is the inlet temperature in °C.

At partial loads, Palmer and Erbes [28] developed the following equation:

$$\dot{m}_{cool} = \dot{m}_{cool,nom} \frac{P}{P_{nom}} \sqrt{\frac{T_{nom}}{T}}, \tag{11}$$

where the subscript *nom* denotes the nominal state.

### 2.1.3. Rankine Cycle

The transformation of the steam’s enthalpy into mechanical energy is performed by the steam turbine. Hence, the enthalpy before and after the turbine is used in computing the efficiency and the nominal values. The steam turbine converts the steam’s enthalpy into mechanical energy. Therefore, the enthalpy is determined by calculating the enthalpy value before the turbine unit, as well as the output and the marginal values after the turbine unit. The mechanical power generated at one end of the turbine transfers to the electrical generator. In the momentum and energy computations, the pressure and enthalpy drops are added as source terms. The pressure drop is a function of the nominal mass flow rate  $\dot{m}_{nom}$  at the turbine inlet nominal pressure  $p_{inl,nom}$  and the turbine outlet’s nominal pressure  $p_{out,nom}$ .

$$\dot{m}_{inl} = \dot{m}_{nom} \frac{p_{inl}}{p_{inl,nom}} \sqrt{\frac{1 - \left(\frac{p_{out}}{p_{inl}}\right)^{\frac{n+1}{n}}}{1 - \left(\frac{p_{out,nom}}{p_{inl,nom}}\right)^{\frac{n+1}{n}}}}. \tag{12}$$

$$n = \frac{\ln\left(\frac{p_{out}}{p_{inl}}\right)}{\ln\left(\frac{p_{out}}{p_{inl}}\right) - \ln\left(\frac{T_{out}}{T_{inl}}\right)}. \tag{13}$$

The specific enthalpy drop in a turbine is computed using Equation (14) in the situation when the fluid is steam.

$$\Delta h_{turb,st} = \left( h_{inl,st} - h_{ref} \right) - \left( h_{out,st} - h_{ref} \right). \tag{14}$$

The specific enthalpy drop is computed using Equation (15) in the situation when there are water droplets in the fluid.

$$\Delta h_{turb,dro} = x \left[ \left( h_{inl,st} - h_{ref} \right) - \left( h_{out,st} - h_{ref} \right) \right] + (1 - x) \left( h(p)_{inl,dro} - h(p)_{out,dro} \right). \quad (15)$$

#### 2.1.4. Ammonia Heat Pump

The use of naturally occurring and environmentally friendly substances as working fluids in heat pump systems helps keep the environment safe. Ammonia and hydrocarbons remain one of the most important natural working fluids. Ammonia heat pumps, therefore, provide an energy-efficient alternative for both heating and cooling for residential applications such as space heating, as well as heating nonresidential buildings. As shown in the system model of Figure 1, the ammonia heat pump consists of four main elements:

**Evaporator:** Heat is received from the heat source and, through the regulation of the evaporator pressure with that of the expansion valve, ensures that, at the desired temperature, the cooling agent begins to boil.

**Compressor:** This increases the pressure in the heat pump system, thereby raising the temperature of the liquid vapor.

**Condenser:** In this element of the heat pump system, the cooling agent provides heat to the internal heating system, which is generally a water circulation system of heat supply to the radiators, in addition to the system supplying hot water.

**Expansion valve or throttle valve or pressure regulator:** This lowers the pressure and removes the cooling agent back to the evaporator, totally changing it into a liquid state so that it can pick up the heat once more [29].

These are the four main parts of the ammonia heat pump, which are designed to be connected through a closed piping system. Ammonia, which is the cooling agent, does not harm the environment.

The COP for the heat pump system is expressed as

$$COP = \frac{\dot{Q}_c}{\dot{W}_{in}}, \quad (16)$$

where  $\dot{Q}_c$  is the amount of heat is transferred to or from a cold reservoir, and  $\dot{W}_{in}$  is the work supplied in moving heat from the cold reservoir to the hot reservoir.

Therefore, for the proposed system, the COP for the heat pump cycle is calculated as

$$COP = \frac{\dot{Q}_{con, hp}}{\dot{W}_{comp, hp}}, \quad (17)$$

where  $\dot{Q}_{con, hp}$  represents the energy output of the condenser of the heat pump, and  $\dot{W}_{comp, hp}$  represents the work performed by the compressor of the heat pump.

#### 2.2. Exergy and Exergoenvironmental Analysis

The condition when the maximum useful work of a system is obtained when a system reversibly reaches equilibrium with its environment is termed exergy. Exergy is widely preferred in the analysis of the performance of thermodynamic systems because it deals with the quality rather than the quantity of energy, which enables losses and inefficiencies to be evaluated realistically [30].

The chemical exergy of the methane fuel can be determined using the exergy ratio relation,

$$\Phi_{CH_4} = \frac{ex_f}{LHV_{CH_4}}, \quad (18)$$

where  $\Phi_{CH_4} = 1.06$  [31], and  $LHV_{CH_4} = 50,023$  kJ/kg.

The exergy balance of the combustion chamber is given as

$$\dot{Q}_{CC} \left( 1 - \frac{T_0}{T_3} \right) + \dot{m}_1 ex_1 + \dot{m}_f ex_f = (\dot{m}_f + \dot{m}_1) ex_3 + \dot{E}x_{D,CC}, \tag{19}$$

where  $\dot{Q}_{CC}$  is the heat output of the combustion chamber,  $\dot{m}_f$  is the mass flow rate of the fuel, and  $\dot{E}x_{D,CC}$  is the exergy destruction in the combustion chamber. The exergy efficiency of the combustion chamber is calculated using

$$\psi_{CC} = \frac{\dot{E}x_4}{\dot{E}x_2 + \dot{E}x_3}. \tag{20}$$

The exergy destruction rate of the other components in the multigeneration system can be obtained using the energy balance equations presented in Table 1.

**Table 1.** Exergy relations for the exergy analysis of the system’s components.

| Component                     | Exergy Balance   |
|-------------------------------|--|
| Air compressor                | $\dot{E}x_1 + \dot{W}_{gas,comp} = \dot{E}x_2 + \dot{E}x_{D,gas,comp}$               |
| Gas turbine                   | $\dot{E}x_5 = \dot{E}x_6 + \dot{W}_{gas,turb} + \dot{E}x_{D,gas,turb}$               |
| Heat recovery steam generator | $\dot{E}x_6 + \dot{E}x_{12} = \dot{E}x_7 + \dot{E}x_8 + \dot{E}x_{D,hrs}$            |
| Steam turbine                 | $\dot{E}x_8 = \dot{E}x_9 + \dot{W}_{steam,turb} + \dot{E}x_{D,steam,turb}$           |
| Condenser 1                   | $\dot{E}x_{10} + \dot{E}x_{18} = \dot{E}x_{11} + \dot{E}x_{19} + \dot{E}x_{D,cond1}$ |
| Pump                          | $\dot{E}x_{11} + \dot{W}_{pump} = \dot{E}x_{12} + \dot{E}x_{D,pump}$                 |
| Evaporator                    | $\dot{E}x_7 + \dot{E}x_{16} = \dot{E}x_{13} + \dot{E}x_{17} + \dot{E}x_{D,evap}$     |
| Ammonia compressor            | $\dot{E}x_{13} + \dot{W}_{NH3,comp} = \dot{E}x_{14} + \dot{E}x_{D,NH3,comp}$         |
| Condenser 2                   | $\dot{E}x_{14} + \dot{E}x_{20} = \dot{E}x_{15} + \dot{E}x_{21} + \dot{E}x_{D,cond2}$ |

An exergoenvironmental analysis of a system is used to measure the impact of the system on the environment. The six parameters used are described below.

Exergoenvironmental impact factor ( $f_{ei}$ ): This shows how a system’s environmental impact can be reduced by decreasing its irreversibility. It is determined using

$$f_{ei} = \frac{\dot{E}x_{dest,tot}}{\dot{E}x_{in}}, \tag{21}$$

where  $\dot{E}x_{dest,tot}$  and  $\dot{E}x_{in}$  represent total exergetic destruction in the system and the overall exergetic destruction supplied to the system.

Exergoenvironmental impact coefficient ( $C_{ei}$ ): The value of  $C_{ei}$  for an ideal case of a system is one to show that there is no exergy destruction. This is defined as

$$C_{ei} = \frac{1}{\eta_{ex}/100}, \tag{22}$$

where  $\eta_{ex}$  is the exergetic efficiency of the system.

Exergoenvironmental impact index ( $\theta_{ei}$ ): This is used to indicate how much damage a system exerts on the environment as a result of its exergy losses and exergy destruction. It is calculated as

$$\theta_{ei} = f_{ei} \times C_{ei}. \tag{23}$$

Exergoenvironmental impact improvement ( $\theta_{eii}$ ): Reducing the exergoenvironmental impact index of a system will increase how appropriate the system is to the environ-

ment. Therefore, the exergoenvironmental improvement of a system is derived from its exergoenvironment impact index using

$$\theta_{eii} = \frac{1}{\theta_{ei}}. \quad (24)$$

Exergy stability factor ( $f_{es}$ ): A system is considered a stable one if its exergy stability factor is close to one. It is defined as

$$f_{es} = \frac{\dot{E}x_{tot,out}}{\dot{E}x_{tot,out} + \dot{E}x_{des,out}}, \quad (25)$$

where  $\dot{E}x_{tot,out}$  represents the desired output exergy.

Exergetic sustainability index ( $\theta_{est}$ ): A system's exergetic sustainability index is a product of its exergy stability factor and its exergoenvironmental impact improvement. It is desired to be as high as possible to illustrate its usefulness to the environment. Its value is derived using

$$\theta_{est} = f_{es} \times \theta_{eii}. \quad (26)$$

### 3. Simulation Scenarios and Results

The parameters for the model inputs used in the simulation are given in Table 2 and the results obtained from the simulation using the input parameters given in Table 2 are presented in Table 3. The total net output of the system is 24,748 kW and the heat pump supplies 1385 kW of heat. The efficiency of the Brayton, Rankine, and overall cycles is 33%, 36%, and 62%, respectively. Furthermore, parametric studies are carried out to demonstrate the performance of the system through the variation of some design parameters for better performance analysis and the results are presented in this section.

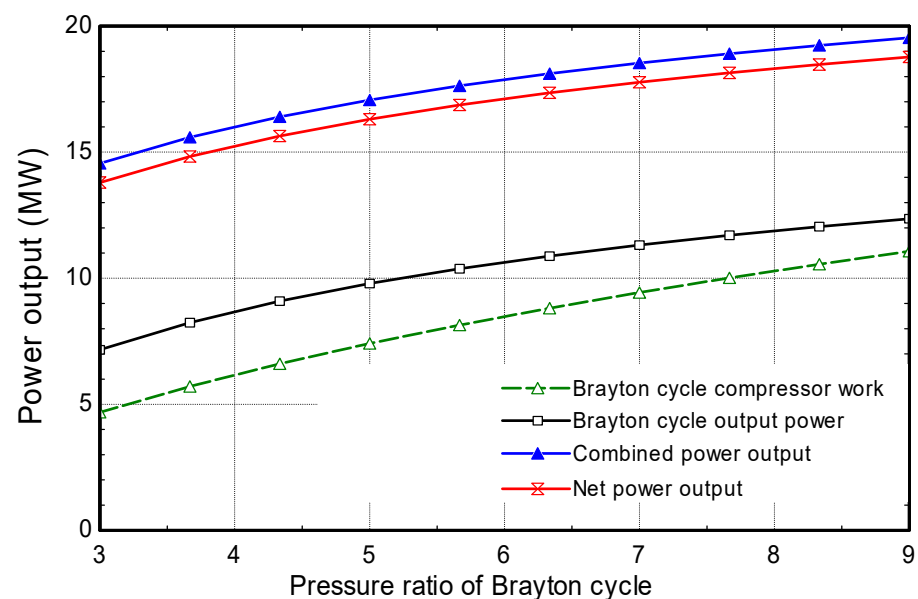
**Table 2.** Input variables used in the simulation.

| Parameter  | Value  | Unit |
|--|--------|------|
| Pressure ratio of Brayton cycle                      | 5      |      |
| Pressure ratio of heat pump                          | 2      |      |
| Inlet pressure of Brayton cycle compressor           | 100    | kPa  |
| Outlet pressure of Rankine cycle pump                | 10,000 | kPa  |
| Efficiency of gas turbine, steam turbine, and pump   | 85     | %    |
| Mass flow rate of Brayton cycle compressor inlet air | 40.92  | kg/s |
| Mass flow rate of Rankine cycle steam                | 4.6    | kg/s |
| Mass flow rate of ammonia in the heat pump           | 3      | kg/s |

**Table 3.** Results obtained from the simulation.

| Parameter                               | Value | Unit |
|---|-------|------|
| Brayton cycle compressor work           | 7.41  | MW   |
| Inlet combustion energy rate            | 29.91 | MW   |
| Brayton cycle net power output          | 9.79  | MW   |
| Rankine cycle pump work                 | 0.56  | MW   |
| Rankine cycle net power output          | 7.50  | MW   |
| Heat pump compressor work               | 0.15  | MW   |
| Heat pump output                        | 1.39  | MW   |
| Net power generated by the system       | 24.75 | MW   |
| Efficiency of Brayton cycle             | 33    | %    |
| Efficiency of Rankine cycle             | 36    | %    |
| COP of heat pump                        | 9.1   |      |
| Overall energy efficiency of the system | 62    | %    |
| Overall exergy efficiency of the system | 78    | %    |

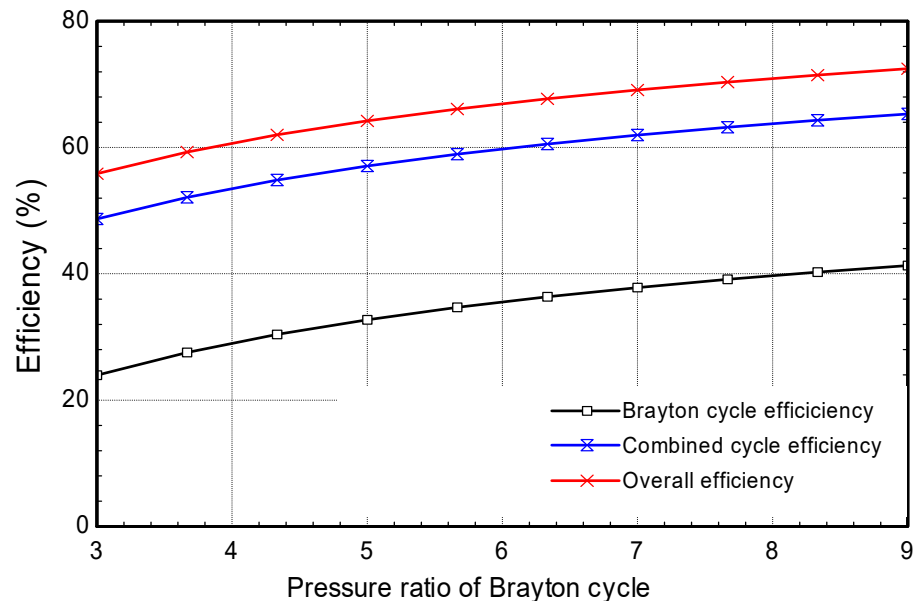
The impact of using different pressure ratios in the Brayton cycle on the compressor work, output power of the Brayton cycle, the combined power output of the Brayton and Rankine cycles, and overall power output is observed in Figure 2. An increase in the pressure ratio from 3 to 9 causes the compressor work to increase from 4.7 MW to 11.1 MW; this is because the compressor will have to perform more work to increase the exit pressure of the air after passing through it. The net power output from the Brayton cycle increases from 7.2 MW to 12.3 MW, while the power output from the combined Brayton and Rankine cycles increases from 14.6 MW to 19.6 MW. The net power output of the overall system is derived by subtracting the amount of work needed to drive the compressor of the heat pump compressor from the net power output of the combined power cycles. Figure 2 shows that increasing the Brayton cycle pressure ratio increases the overall net power output from 13.9 MW to 18.8 MW; this is because of the immense increase in the power output from the Brayton cycle which nearly doubles in value.



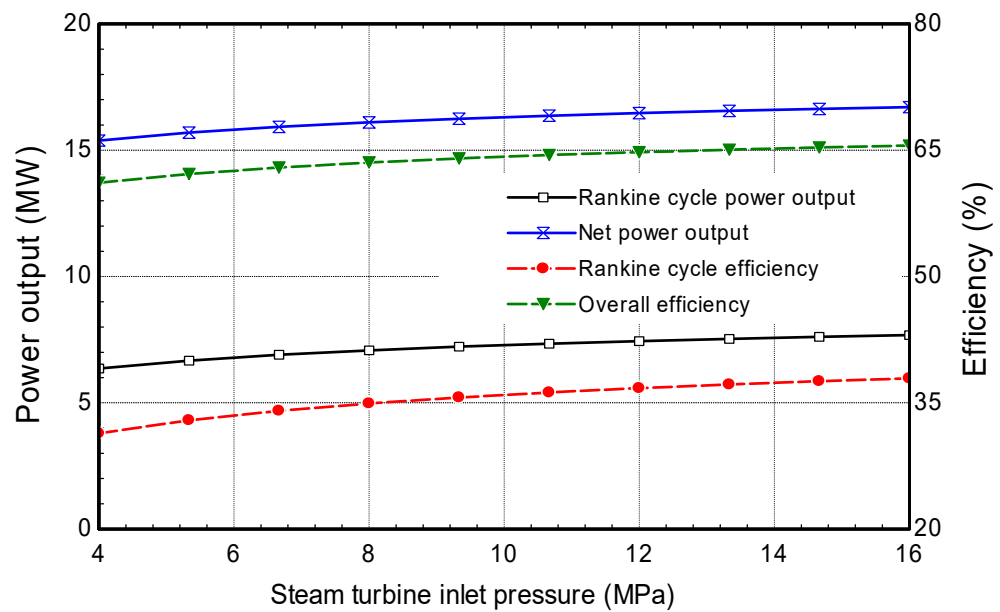
**Figure 2.** Impact of varying the pressure ratio of the Brayton cycle on the compressor work and power output.

Figure 3 explains the impact of the variation of the pressure ratio on the efficiencies of the Brayton cycle, the combined cycle, and the overall system. The effects observed in Figure 3 mirror those presented in Figure 2. For an increase in the pressure ratio from 3 to 9, the Brayton cycle efficiency increases from 24% to 42%. Moreover, the efficiency of the combined power cycles increases from 49% to 66%. It should be noted that combining a simple Rankine cycle to recover the exhaust heat from the Brayton cycle increases the combined cycle efficiency by about 25% compared to the Brayton cycle alone. The efficiency of the overall system also increases from 56% to 73%.

Figure 4 examines the effect of varying the inlet pressure of the steam turbine on the steam turbine performance and the overall combined system performance. It can be observed that increasing the steam turbine inlet pressure from 4 MPa to 16 MPa leads to an increment in the net power output of the Rankine cycle from 6.5 MW to 7.7 MW. The net power output of the total system increases from 15.4 MW to 16 MW. This increase in the steam turbine inlet pressure also increases both the efficiency of the Rankine cycle and the efficiency of the overall system. The steam cycle efficiency increases from 31% to 38% while the overall efficiency increases from 62% to 66%.



**Figure 3.** Impact of varying the pressure ratio of the Brayton cycle on the Brayton cycle efficiency, combined cycle efficiency, and the efficiency of the overall system.



**Figure 4.** Impact of varying the inlet pressure of the steam turbine on the Rankine cycle output power, Rankine cycle efficiency, net power output, and the efficiency of the overall system.

The impact of varying the pressure ratio of the heat pump on its compressor work, the heat pump output, and the COP of the heat pump is illustrated in Figure 5. An increase in the pressure ratio from 1.8 to 3 causes an increase in all the parameters considered. The heat pump compressor work increases from 0.13 MW to 0.29 MW, and the heat pump output increases from 1.37 MW to 1.53 MW. The COP of the heat pump, however, decreases from 11 to 5.3. The resultant changes in the Brayton cycle power output, the combined power output, the net power output of the overall system, and the heat pump output energy are shown in Figure 6 when the combustion inlet energy rate is varied. It can be observed that increasing the combustion inlet energy rate from 25 MW to 35 MW causes an increase in the output energy rate of all the systems. The heat pump output energy rate increases from 1.38 MW to 1.39 MW, while the Brayton cycle experiences an increase in power output from

8.2 MW to 11.5 MW. The overall power output from the multigeneration system increases from 15.5 MW to 19 MW.

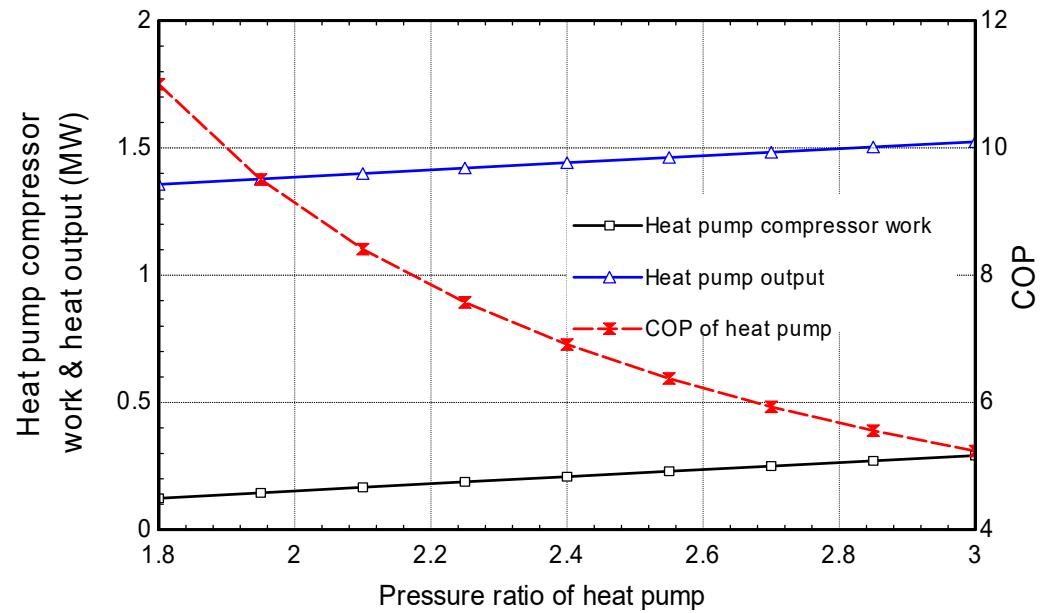


Figure 5. Impact of varying the pressure ratio of the heat pump on the compressor work of the heat pump, the heat pump output, and the COP of the heat pump.

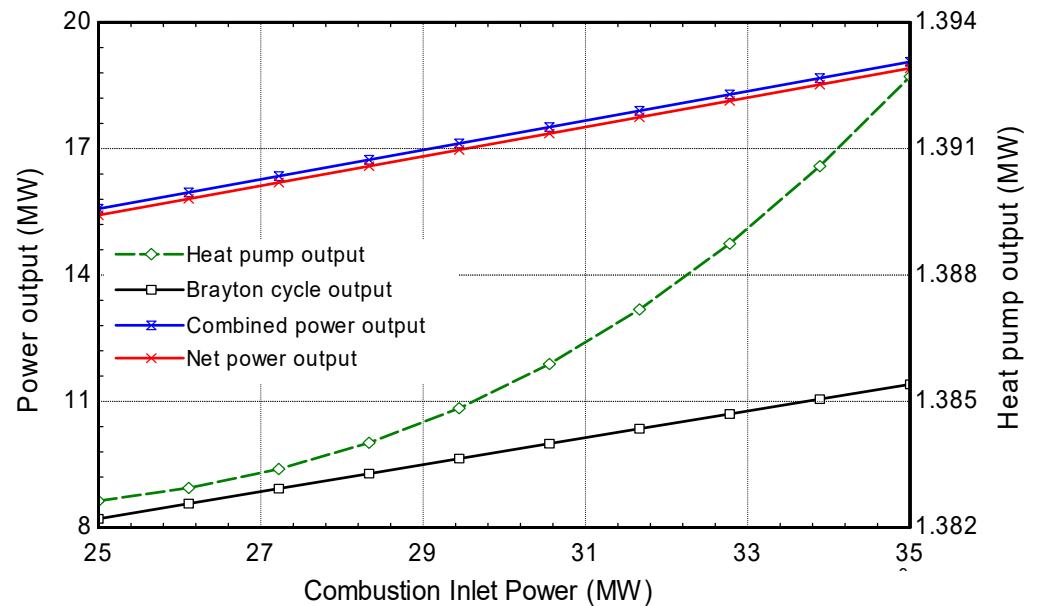


Figure 6. Impact of varying the combustion inlet energy rate on the Brayton cycle power output, combined power output, heat pump output, and the net power output of the overall system.

The effect of varying the inlet energy rate from the combustion chamber on the  $f_{ei}$  and  $C_{ei}$  is presented in Figure 7. While the  $f_{ei}$  decreases from about 0.51 to 0.3, the  $C_{ei}$  can be seen to decrease from 2.05 to 0.6. The decreasing nature of both factors is a good indicator of the system's reduced environmental impact, and this also shows that the system's irreversibility is decreasing. Figure 8 shows the effect of varying the inlet energy rate from the combustion chamber on  $\theta_{ei}$  and  $\theta_{eii}$  of the system. The  $\theta_{ei}$  decreases from about 1.0 to 0.1, while the  $\theta_{eii}$  increases from 1.05 to 6.1. The value of  $\theta_{ei}$  for a system should be as low as possible, while a high  $\theta_{eii}$  indicates that the system is beneficial to the environment. The effect of increasing inlet energy rate on the exergy stability factor and

exergetic sustainability index of the system can be seen in Figure 9. The  $f_{es}$  increases from 0.41 to 0.47, while the  $\theta_{est}$  also increases from about 0.6 to 0.64. The factors increasing point to the conclusion about the stability and sustainability of the system upon increasing the inlet combustion energy rate.

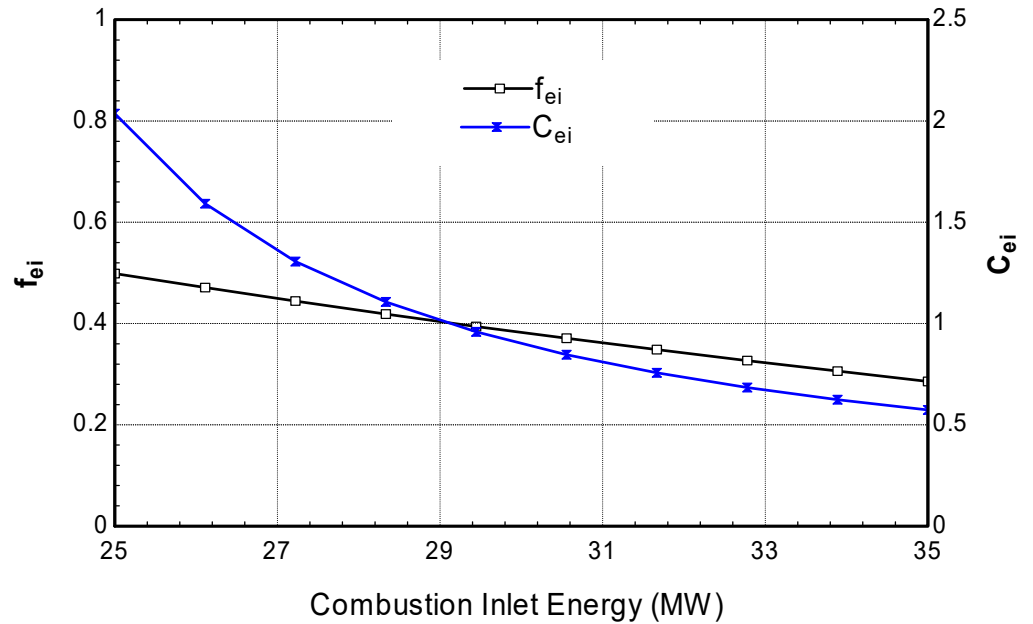


Figure 7. Impact of varying the combustion inlet energy rate on the exergoenvironmental impact factor and exergoenvironmental impact index of the overall system.

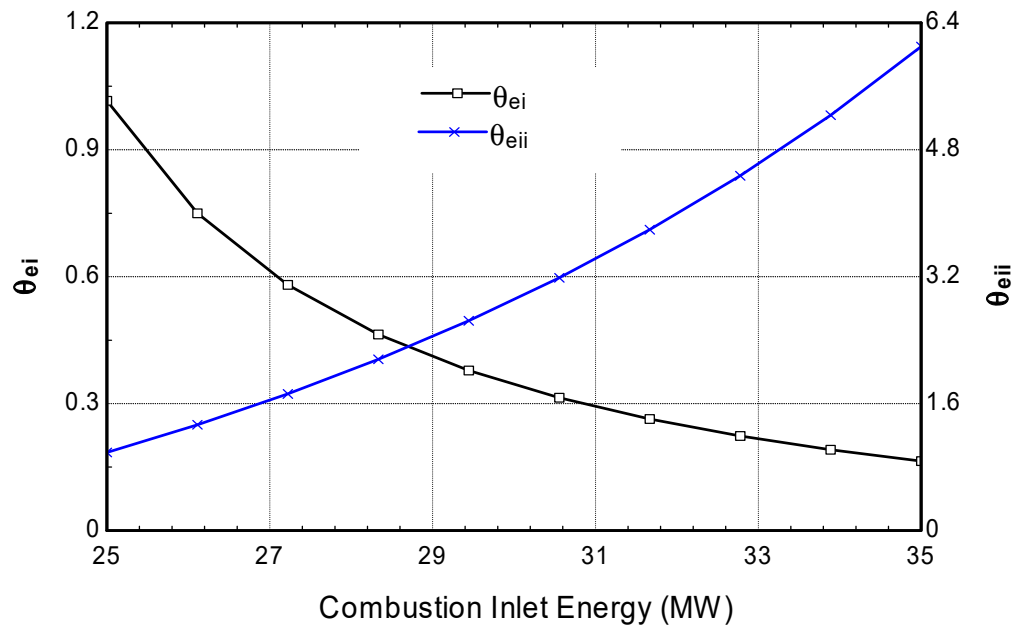
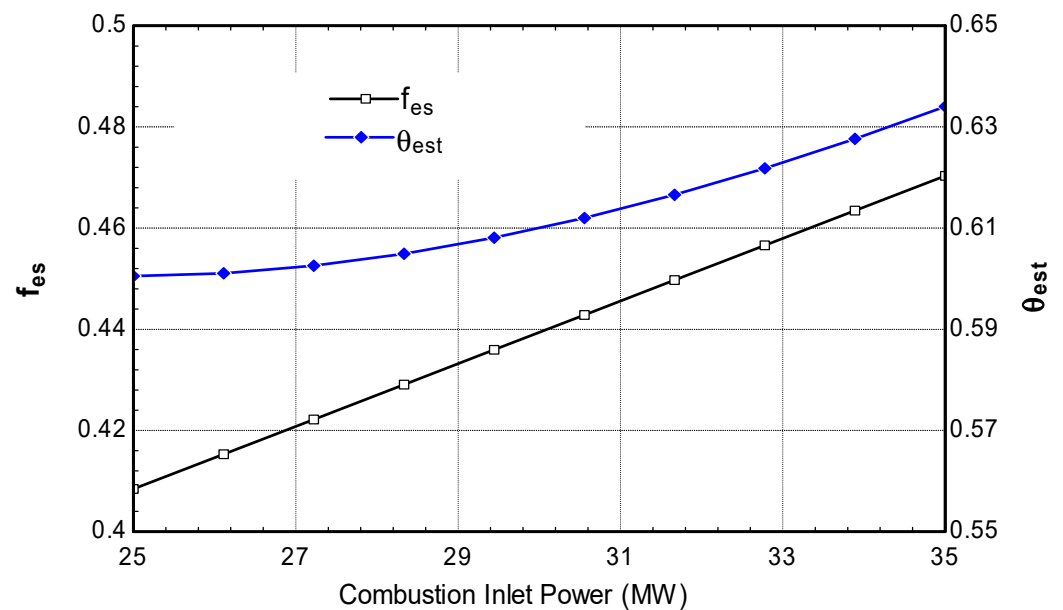


Figure 8. Impact of varying the combustion inlet energy rate on the environmental impact index and the environmental impact factor of the overall system.



**Figure 9.** Impact of varying the combustion inlet energy rate on the exergy stability factor and exergetic sustainability index of the overall system.

The exergy destruction rate of each component of the system as a percentage of the overall exergy destruction rate is displayed in Table 4. It is seen that over 50% of the exergy destruction in the system occurs in the combustion chamber; this is reflective of systems which operate on fuel combustion of any kind. The large range of temperature difference of the chemical and heat transfer between the working fluid and the methane fuel causes high levels of exergy destruction in the combustion chamber [32]; improving this multigeneration system significantly will require the fuel combustion process to be thoroughly improved.

**Table 4.** Exergy destruction for each component in the system.

| Component          | Exergy Destruction Rate (kW) | Share of Total (%) |
|--------------------|------------------------------|--------------------|
| Compressor 1       | 137.3                        | 2.8                |
| Combustion chamber | 2774.5                       | 56.6               |
| Turbine 1          | 465.7                        | 9.5                |
| HRSG               | 500.0                        | 10.2               |
| Turbine 2          | 176.5                        | 3.6                |
| Condenser 1        | 529.4                        | 10.8               |
| Pump               | 14.7                         | 0.3                |
| Evaporator         | 88.2                         | 1.8                |
| Compressor 2       | 117.6                        | 2.4                |
| Condenser 2        | 93.1                         | 1.9                |
| Valve              | 4.9                          | 0.1                |
| Total              | 4902                         | 100                |

#### 4. Conclusions

In this paper, a combined cycle power plant was analyzed to observe the performance of a combined gas and steam power plant under varied component parameters. The proposed system was modelled using the Thermolib extension library in MATLAB. The results obtained from the system gave the net power from the Brayton cycle, Rankine cycle and overall system as 7.41 MW, 29.91 MW, and 24.75 MW respectively. The efficiencies were found to be 33%, 36%, and 62% respectively. The overall exergy efficiency of the multigeneration system was calculated as 78%. The ammonia heat pump had an output of 1.39 MW with a COP of 9.1.

The outcome of the study showed that using different pressure ratios ultimately affected the gas cycle and the overall system performance, as it increased the gas turbine compressor work, gas turbine output power, the net power output, and the overall efficiency of the system. Increasing the pressure ratio of the Brayton cycle from 3 to 9 increased the Brayton cycle output power from 7.2 MW to 12.3 MW, while the net power output increased from 13.9 MW to 18.8 MW. Varying the pressure ratio also increased the efficiency of the Brayton cycle from 24% to 42%, while the combined efficiency of both the Brayton cycle and the Rankine cycle increased from 49% to 66%. Increasing the steam turbine inlet pressure from 4 MPa to 16 MPa increased the Rankine cycle power output from 6.5 MW to 7.7 MW, while the overall efficiency of the system increased from 62% to 66%. The heat flow rate into the combustion chamber also varied from 25 MW to 35 MW, and this caused the net power output of the system to increase from 15.5 MW to 19 MW. The exergoenvironmental analysis of the system showed the appropriateness, usefulness, and stability of the multigeneration system in the environment.

The effect of varying the combustion inlet energy rate on the exergoenvironmental impact of the overall system was also analyzed. The results showed favorable exergoenvironmental effects, indicating a reduction in the system's overall irreversibility and environmental impact, made possible by the improved combustion efficiency in the combustion chamber.

**Author Contributions:** Formal analysis, H.A.; Investigation, M.A. (Michael Adedeji); Methodology, M.A. (Mohammed Abid) and D.A.; Supervision, J.H.Z.; Writing—original draft, H.A. (Humphrey Adun) and D.A.; Writing—review & editing, A.T.O. All authors have read and agreed to the published version of the manuscript.

**Funding:** This work is funded by Universiti Brunei Darussalam, under the grant # UBD/RSCH/1.3/FICBF(b)/2022/017.

**Institutional Review Board Statement:** Not applicable.

**Informed Consent Statement:** Not applicable.

**Data Availability Statement:** Not applicable.

**Conflicts of Interest:** The authors declare no conflict of interest.

## Nomenclature

|               |   |
|---------------|---|
| COP           | Coefficient of performance                  |
| CHP           | Combined heat and power                     |
| $C_p$         | Specific heat at constant pressure, kJ/kg·K |
| EES           | Engineering equation solver                 |
| $\dot{E}_x$   | Exergy rate                                 |
| h             | Enthalpy                                    |
| HRSG          | Heat recovery steam generator               |
| $\dot{Q}$     | Heat rate, kW                               |
| $\dot{m}$     | Mass flow rate, kg/s                        |
| $\dot{W}$     | Work rate, kW                               |
| T             | Temperature, °C                             |
| Greek letters |   |
| $\eta$        | Efficiency                                  |
| $\Delta$      | Difference                                  |
| $\Phi$        | Exergy ratio                                |
| Subscripts    |   |
| c             | Cold reservoir                              |
| comp          | Compressor                                  |
| D             | Destruction                                 |
| dro           | Water droplets                              |

|      |            |
|------|------------|
| fg   | Flue gas   |
| inl  | Inlet      |
| isen | Isentropic |
| nom  | Nominal    |
| out  | Outlet     |
| turb | Turbine    |
| ref  | Reference  |
| hp   | Heat pump  |
| st   | Steam      |

## References

- Rosen, M.; Dincer, I.; Kanoglu, M. Role of exergy in increasing efficiency and sustainability and reducing environmental impact. *Energy Policy* **2008**, *36*, 128–137. [\[CrossRef\]](#)
- Dincer, I.; Rosen, M. *Exergy: Energy, Environment and Sustainable Development*, 2nd ed.; Elsevier Science: Oxford, UK, 2012.
- Kaviri, A.G.; Jaafar, M.N.M.; Lazim, T.M.; Barzegaravval, H. Exergoenvironmental optimization of Heat Recovery Steam Generators in combined cycle power plant through energy and exergy analysis. *Energy Convers. Manag.* **2013**, *67*, 27–33. [\[CrossRef\]](#)
- Karklina, K.; Cimdina, G.; Veidenbergs, I.; Blumberga, D. Energy and Exergy Analysis of Wood-based CHP. Case Study. *Energy Procedia* **2016**, *95*, 507–511. [\[CrossRef\]](#)
- Ahmadi, P.; Rosen, M.A.; Dincer, I. Greenhouse gas emission and exergo-environmental analyses of a trigeneration energy system. *Int. J. Greenh. Gas Control* **2011**, *5*, 1540–1549. [\[CrossRef\]](#)
- Cavalcanti, E.J.C.; Ferreira, J.V.M.; Carvalho, M. Research on a solar hybrid trigeneration system based on exergy and exergoenvironmental assessments. *Energies* **2021**, *14*, 7560. [\[CrossRef\]](#)
- Abdul Hussain Ratlamwala, T.; Dincer, I.; Gadalla, M. Comparative Environmental Impact and Sustainability Assessments of Hydrogen and Cooling Production Systems. In *Causes, Impacts and Solutions to Global Warming*, 1st ed.; Springer: New York, NY, USA, 2013; pp. 389–408.
- Xia, J.; Chen, G.; Tan, P.; Zhang, C. An online case-based reasoning system for coal blends combustion optimization of thermal power plant. *Int. J. Electr. Power Energy Syst.* **2014**, *62*, 299–311. [\[CrossRef\]](#)
- Alobaid, F.; Postler, R.; Ströhle, J.; Epple, B.; Kim, H.G. Modeling and investigation start-up procedures of a combined cycle power plant. *Appl. Energy* **2008**, *85*, 1173–1189. [\[CrossRef\]](#)
- Starkloff, R.; Alobaid, F.; Karner, K.; Epple, B.; Schmitz, M.; Boehm, F. Development and validation of a dynamic simulation model for a large coal-fired power plant. *Appl. Therm. Eng.* **2015**, *91*, 496–506. [\[CrossRef\]](#)
- Kim, J.H.; Kim, T.S.; Ro, S.T. Analysis of the dynamic behaviour of regenerative gas turbines. *Proc. Inst. Mech. Eng. Part A J. Power Energy* **2001**, *215*, 339–346. [\[CrossRef\]](#)
- Alobaid, F.; Starkloff, R.; Pfeiffer, S.; Karner, K.; Epple, B.; Kim, H.G. A comparative study of different dynamic process simulation codes for combined cycle power plants—Part A: Part loads and off-design operation. *Fuel* **2015**, *153*, 692–706. [\[CrossRef\]](#)
- Alobaid, F.; Starkloff, R.; Pfeiffer, S.; Karner, K.; Epple, B.; Kim, H.G. A comparative study of different dynamic process simulation codes for combined cycle power plants—Part B: Start-up procedure. *Fuel* **2015**, *153*, 707–716. [\[CrossRef\]](#)
- Maffezzoni, C. Issues in Modelling and Simulation of Power Plants. *IFAC Proc.* **1992**, *25*, 15–23. [\[CrossRef\]](#)
- Lu, S. Dynamic modelling and simulation of power plant systems. *Proc. Inst. Mech. Eng. Part A J. Power Energy* **1999**, *213*, 7–22. [\[CrossRef\]](#)
- Colonna, P.; van Putten, H. Dynamic modeling of steam power cycles.: Part I—Modeling paradigm and validation. *Appl. Therm. Eng.* **2007**, *27*, 467–480. [\[CrossRef\]](#)
- van Putten, H.; Colonna, P. Dynamic modeling of steam power cycles: Part II—Simulation of a small simple Rankine cycle system. *Appl. Therm. Eng.* **2007**, *27*, 2566–2582. [\[CrossRef\]](#)
- Celis, C.; Pinto, G.R.S.; Teixeira, T.; Xavier, É. A steam turbine dynamic model for full scope power plant simulators. *Appl. Therm. Eng.* **2017**, *120*, 593–602. [\[CrossRef\]](#)
- Okon, E.; Wang, M. Dynamic modelling, validation and analysis of coal-fired subcritical power plant. *Fuel* **2014**, *135*, 292–300. [\[CrossRef\]](#)
- Wang, C.; Liu, M.; Li, B.; Liu, Y.; Yan, J. Thermodynamic analysis on the transient cycling of coal-fired power plants: Simulation study of a 660 MW supercritical unit. *Energy* **2017**, *122*, 505–527. [\[CrossRef\]](#)
- Powell, K.M.; Edgar, T.F. Modeling and control of a solar thermal power plant with thermal energy storage. *Chem. Eng. Sci.* **2012**, *71*, 138–145. [\[CrossRef\]](#)
- Xu, E.; Wang, Z.; Wei, G.; Zhuang, J. Dynamic simulation of thermal energy storage system of Badaling 1 MW solar power tower plant. *Renew Energy* **2012**, *39*, 455–462. [\[CrossRef\]](#)
- Chen, C.; Zhou, Z.; Bollas, G.M. Dynamic modeling, simulation and optimization of a subcritical steam power plant. Part I: Plant model and regulatory control. *Energy Convers. Manag.* **2017**, *145*, 324–334. [\[CrossRef\]](#)
- Liu, M.; Steven Tay, N.H.; Bell, S. Review on concentrating solar power plants and new developments in high temperature thermal energy storage technologies. *Renew. Sustain. Energy Rev.* **2016**, *53*, 1411–1432. [\[CrossRef\]](#)

25. Moran, M.J.; Shapiro, H.N. *Fundamentals of Engineering Thermodynamics*, 4th ed.; John Wiley: Hoboken, NJ, USA, 2000.
26. Casella, F.; Colonna, P. Dynamic modeling of IGCC power plants. *Appl. Therm. Eng.* **2012**, *35*, 91–111. [[CrossRef](#)]
27. Alobaid, F.; Mertens, N.; Starkloff, R.; Lanz, T.; Heinze, C.; Epple, B. Progress in dynamic simulation of thermal power plants. *Prog. Energy Combust. Sci.* **2017**, *59*, 79–162. [[CrossRef](#)]
28. Karimi, I.A. *Impact of Control Strategies on the Off-Design Operation of the Gas Turbine in a Combined Cycle Gas Turbine (Ccgt) Power*; 2011. Available online: [folk.ntnu.no/skoge/prost/proceedings/focapo-cpc-2017/FOCAPO-CPC%2017%20contributed%20papers/108\\_FOCAPO\\_Contributed.pdf](http://folk.ntnu.no/skoge/prost/proceedings/focapo-cpc-2017/FOCAPO-CPC%2017%20contributed%20papers/108_FOCAPO_Contributed.pdf) (accessed on 5 July 2022).
29. Chua, K.J.; Chou, S.K.; Yang, W.M. Advances in heat pump systems: A review. *Appl. Energy*. **2010**, *87*, 3611–3624. [[CrossRef](#)]
30. Terzi, R. Application of Exergy Analysis to Energy Systems. In *Application of Exergy*; IntechOpen: London, UK, 2018.
31. Ahmadi, P.; Dincer, I.; Rosen, M.A. Exergy, exergoeconomic and environmental analyses and evolutionary algorithm based multi-objective optimization of combined cycle power plants. *Energy* **2011**, *36*, 5886–5898. [[CrossRef](#)]
32. Dincer, I.; Rosen, M.A. *Exergy*, 2nd ed.; Elsevier: Oxford, UK, 2000.